



In Situ Imaging and Structure Determination of Biomolecular Complexes Using Electron Cryo-Tomography

Mohammed Kaplan, William J. Nicolas, Wei Zhao, Stephen D. Carter, Lauren Ann Metskas, Georges Chreifi, Debnath Ghosal, and Grant J. Jensen

Abstract

Electron cryo-tomography (cryo-ET) is a technique that allows the investigation of intact macromolecular complexes while they are in their cellular milieu. Over the years, cryo-ET has had a huge impact on our understanding of how large biomolecular complexes look like, how they assemble, disassemble, function, and evolve(d). Recent hardware and software developments and combining cryo-ET with other techniques, e.g., focused ion beam milling (FIB-milling) and cryo-light microscopy, has extended the realm of cryo-ET to include transient molecular complexes embedded deep in thick samples (like eukaryotic cells) and enhanced the resolution of structures obtained by cryo-ET. In this chapter, we will present an outline of how to perform cryo-ET studies on a wide variety of biological samples including prokaryotic and eukaryotic cells and biological plant tissues. This outline will include sample preparation, data collection, and data processing as well as hybrid approaches like FIB-milling, cryosectioning, and cryo-correlated light and electron microscopy (cryo-CLEM).

Key words Cryo-ET, In situ structural biology, Subtomogram averaging, FIB-milling, High-resolution tomography, Cryosectioning

1 Introduction

The continuous interaction of proteins with each other, and with other molecules, in the crowded environment of the cell generates life. Disentangling the structure and dynamics of proteins while they are in this native milieu is crucial to structural biology. To achieve this, multiple imaging and spectroscopic techniques have been developed in recent years that aim at investigating biomolecules at ever higher resolution inside the cell (*see, e.g., Refs. 1–4*). Cryo-ET has now become an indispensable tool to investigate molecular complexes in intact cells in a frozen hydrated state at

nanometer resolution [5, 6]. In favorable cases, atomic models of these nanomachines can be built using known high-resolution structures obtained by other methods like NMR, X-ray crystallography, and single particle analysis (SPA) which provides new mechanistic insights [7]. Moreover, comparing the structures of different nanomachines or of the same nanomachine in different species can shed light on how these biological machines have evolved (and continue evolving) over time [8, 9]. In addition, cryo-ET is very powerful in studying how large complexes assemble and disassemble in the cell and is capable of capturing and revealing the structures of intermediate and transient states during such processes which is crucial in deciphering such pathways [10–13].

Cryo-ET is one of the essential modes of Cryo-EM (together with SPA and Micro-Electron Diffraction (MicroED)) in which a 3D reconstruction of the sample is produced by back-projecting images of the sample taken at different tilt angles. Usually, the sample is tilted from -60° to $+60^\circ$ every 1° – 3° . As biological samples are sensitive to radiation, different tilt-schemes have been developed like the bidirectional tilt-scheme and the dose symmetric tilt-scheme [14] and the selection of a specific tilt-scheme is dependent on the sample and the question to be answered. In many cases, single tomograms may not have sufficient signal to provide a detailed knowledge of the molecular complex of interest. Therefore, to enhance the signal and the resolution of tomography data, subtomogram averaging can be performed whereby the subvolumes in the tomograms that have the complex of interest are cropped, aligned, and then averaged to produce an improved signal-to-noise 3D average of the complex of interest [15, 16]. The final resolution of subtomogram averaging depends on many factors with some of them being related to how the data was collected and others determined by inherent characteristics of the complex of interest (flexibility, thickness heterogeneity, etc.). Currently, by averaging many subvolumes the macromolecular structures of many biological machines have been solved (*see*, e.g., Refs. 8, 10, 12, 17–26). For some samples, atomic models have been generated (e.g., Refs. 27, 28).

Hybrid approaches that combine cryo-ET with other methods have recently extended its applicability and usefulness. This includes cryo-CLEM which allows the localization of specific protein complexes and targeted data collection on only the cells or parts of cells that have the complex of interest. Moreover, as the quality of tomography data depends on the sample thickness, cryo-ET has been limited for a long time to thin samples like bacterial cells or the thin edges of eukaryotic cells. Thicker samples required the cumbersome task of cryosectioning. However, the recent development of FIB-milling has extended the realm of tomography to targets located deep in the thick regions of eukaryotic cells [29]. Finally, recent hardware developments like phase plates

[30], direct electron detection cameras with high quantum efficiency and the development of fast-tilt-series schemes [31] (which decrease the time of data collection significantly) have further extended the reach, power, and resolution of cryo-ET.

In this chapter, we present a general outline of the workflow that we use in our laboratory to investigate different kinds of biological samples with cryo-ET, starting from sample preparation and proceeding through data collection and processing. This discussion will include prokaryotic as well as different types of eukaryotic samples (like plant tissues), hybrid approaches like cryo-ET with cryo-CLEM or FIB-milling or both, and cryosectioning of thick biological samples like plant tissues. Finally, we will comment on the requirements for high-resolution tomography in terms of data processing and data collection, including rapid tilt-series schemes.

This chapter is organized into two major sections which are sample preparation and data collection and processing. In the sample preparation section, we will discuss bacterial samples as an example of single small cells, isolated eukaryotic cells and plant tissues in separate subsections. Finally, one should bear in mind that the steps outlined here represent a general protocol and specific tweaks and modifications might be applied to each sample specifically.

2 Sample Preparation

2.1 *Single Small Cells*

This section is applicable to many types of unicellular small organisms. We will discuss bacterial samples as an example. For a detailed discussion of how to perform tomography on a specific large bacterial protein complex, we refer the reader to our recently published chapter [32].

2.1.1 *Bacterial Cultures*

In general, we start from a $-80\text{ }^{\circ}\text{C}$ glycerol stock of the bacterial strain which is cultured on a suitable agar plate under the required conditions (e.g., temperature, antibiotics, and CO_2). Subsequently, a single colony is inoculated into suitable liquid medium and allowed to grow to the desired OD_{600} . Note that this general workflow can differ for different conditions/strains. For example, it might be sometimes better to grow the cells on an agar plate then resuspend them in a liquid medium just prior to freezing. Therefore, one needs to optimize the growth conditions for the investigated bacterial species and for the specific aim of the experiment.

2.1.2 *Grids and Gold Fiducials*

For many bacterial samples destined for tomography, we use copper R2/2 200 Quantifoil holey extra thick carbon grids. However, if the cells need to be incubated on the grids for a significant amount of time, we recommend gold grids with Quantifoil holey carbon as copper is toxic to the cells. When correlated work between different

kinds of microscopes is required, finder grids may be used to facilitate the process of correlation. Prior to use, the grids are glow-discharged to increase their hydrophilicity. In our lab, the grids are glow-discharged for 60 s with 15 mA negative discharge at 1×10^{-1} bar using an Emitech K100× glow-discharging device. Gold fiducials are coated with bovine serum albumin (BSA) to secure a homogenous dissemination of the beads. In a 1.5 mL Eppendorf tube, 1 mL of gold nanoparticles (generally 10–20 nm in diameter) is mixed with 5% BSA (two such tubes are usually prepared). After that, they are spun down at $14,000 \times g$ for 30 min. The pellets of the two tubes are resuspended in $\sim 80 \mu\text{L}$ of the supernatant. This solution is subsequently diluted (7–8 times) with the bacterial sample prior to freezing. The remaining solution of gold nanoparticles can be kept for many weeks at 4°C . If the fiducial markers aggregate around the cells because of the inherent characteristics of the bacteria (e.g., S-layer or extracellular matrix), they can be laid down on the grids prior to freezing. To do so, proceed as described above but dilute with PBS instead of the bacterial sample. From this diluted solution, pipette $3 \mu\text{L}$ onto each glow-discharged grid held by autoclosing forceps. Incubate the drop for approximately 1 min and carefully back-blot the drop on the other side of the grid, making sure the grid is not damaged. Leave to dry for several minutes. Optional screening under a binocular loupe can ensure the overall integrity of the grid. The grids are then glow-discharged again with the same parameters.

2.1.3 Plunge Freezing of Bacterial Cells

Samples are blotted either manually or automatically in the blotting chamber of the Vitrobot. Temperature is usually kept at 22°C with 100% humidity. The blotting conditions (e.g., humidity, blotting force, and time) have to be identified and optimized for each sample. Once plunge-frozen, samples can be kept in liquid nitrogen dewars for long-term storage.

2.2 Eukaryotic Cells

The choice of cell type is a critical consideration for cryo-ET. For successful cryo-ET imaging of peripheral cellular thin edges and extensions, some types of mammalian cells are better suited and reveal extensively larger imageable areas of cytoplasm. In our experience, U2OS, 3T3, and fibroblasts spread optimally on EM grids to reveal peripheral thin edges that are electron transparent. Otherwise, additional thinning steps, such as FIB-milling (*see* below) may be required to gain access to the thicker regions of the cell body and nucleus.

Choice of grid support is critical. Standard copper EM grids are toxic to cells; therefore, an inert grid material such as gold should be used. For cryo-CLEM work, it is recommended that finder grids with reference markers such as letters, symbols, and numbers be used to easily locate target cells imaged between light microscope (LM) and EM modalities. Here, we include all the steps for a cryo-CLEM workflow.

2.2.1 Preparing Cells

Sample preparation depends on the cell type. Here we give an example for U2OS cells.

U2OS cells should be grown in a T75 flask containing McCoy's 5a Medium Modified (*see Note 1*). Typically, U2OS cells are passaged every 2 days and new media replaced every day. At all times, the cells are incubated at 37 °C with 5% CO₂. The U2OS cells are grown to 80% confluency in a T75 flask before being detached by trypsin and seeded on EM grids. Usually, 1 mL of trypsin is added to the flask and left to incubate at 37 °C for 2 min. Next, 6 mL of media is added to the flask to neutralize the trypsin (*see Note 2*). To remove clumps and achieve a single-cell suspension, the cells are pipetted up and down 20 times using a 10 mL pipette. A cell strainer can also be used to obtain a uniform single-cell suspension from mammalian cells. The suspended cells are then transferred to a 10 mL Falcon tube.

2.2.2 Preparing EM Grids for Tissue Culture

1. London finder grids with Quantifoil holey carbon are UV treated for 1 h before plating experiment (*see Note 3*). Specific extracellular matrix proteins (ECMs) can be used to improve attachment and spreading of various cells. The most commonly used ECMs are collagen, fibronectin, poly-L-lysine, and laminin. For U2OS cells, we use collagen. Several drops of human collagen diluted ten times in H₂O are pipetted onto parafilm.
2. A UV-treated grid is then placed carbon-side down on the drop for 2 min. The grid is then flipped so that the grid sinks to the bottom of the drop with the carbon-side now facing up (*see Note 4*). The grid is left in the drop for 20 min.
3. Once the grid has incubated in the drop, it is picked up with tweezers and the excess collagen solution on the grid is blotted away with Whatman 40 blotting paper and the grid is left to dry.

2.2.3 Growing Mammalian Cells on Grids

1. Glass slides are placed in a 10 mL petri dish and UV treated for 20 min. 20 mLs of media is then added to the petri dish to cover the glass slides. Alternatively, when smaller volumes of samples are required a 35 mm imaging dish with coverslip bottom can be used.
2. The pre-coated EM grids are then submerged into the media of the petri dish with the carbon side of the grid facing upwards and placed on the glass slide.
3. The detached cells are then added to the petri dish. The optimal density for growing cells on R2/2 grids is 1 or 2 cells per grid square. If there are more than three cells per grid square, there will be little room for the cells to spread and grow flat. Plating cells on grids so that roughly one or two cells are present in most of the grid squares can be achieved by

measuring a set density of cells in suspension using a cell counter. Or the trypsinized cells in the 10 mL Falcon tube can simply be pipetted onto the medium above the grids and left to settle into the grid squares. A light microscope can be used to evaluate if a suitable density has been achieved.

4. U2OS cells are grown on the grids for 15–20 h before plunge-freezing.

2.2.4 Freezing Grids, Including Adding 20 nm Gold Beads and Fluorescent Microspheres for Cryo-CLEM

1. The EM grids are taken out of the media with Vitrobot tweezers, which are placed into the Vitrobot (*see Note 5*). Blot the excess media from the grid before adding 3 μ L of 20 nm gold solution and 0.5 μ m TetraSpeck Microspheres (*see Note 6*).
2. We recommend manual blotting from the gold side of the grid with all Vitrobot parameters set to 0. It is recommended that the humidity of the Vitrobot chamber be at 95% when the grid is blotted (*see Notes 7 and 8*).
3. After plunge-freezing, the grids are stored within grid boxes cooled in clean liquid nitrogen.
4. Before cryo-LM or cryo-EM imaging, EM grids are clipped into FEI autogrids.

2.2.5 Cryo-LM Imaging for Cryo-CLEM Using the FEI Cryostage

1. In our setup, an FEI cryostage modified to hold Titan Krios cartridges is used, and liquid nitrogen is continuously pumped into the stage by a Norton cryo-pump to maintain the temperature at 80 K. Wait approximately 40 min for the stage to equilibrate and maintain its cryogenic temperature.
2. Load one grid into the stage at a time.
3. Collect a montage or a series of individual phase contrast and fluorescent Z-stack images of mammalian cells growing flat within the grid square and near the center of the grid (Fig. 1). If your target protein is tagged with a green fluorescent protein (GFP) (*see Note 9*), collection of red, blue, and green fluorescent images is recommended (*see Note 10*).
4. Evaluation of ice thickness should be made when imaging mammalian cells using cryo-LM. Ice cracks and thick ice around the circumference of the square are indications that the ice is too thick around the cell. In addition, obvious cracks in the carbon support close to target cells are not ideal and will affect the stability of the cell when being tilted, which can lead to suboptimal tilt-series alignment.
5. Align the fluorescent images to the fluorescent microspheres observed in the phase contrast image (*see Note 11*).

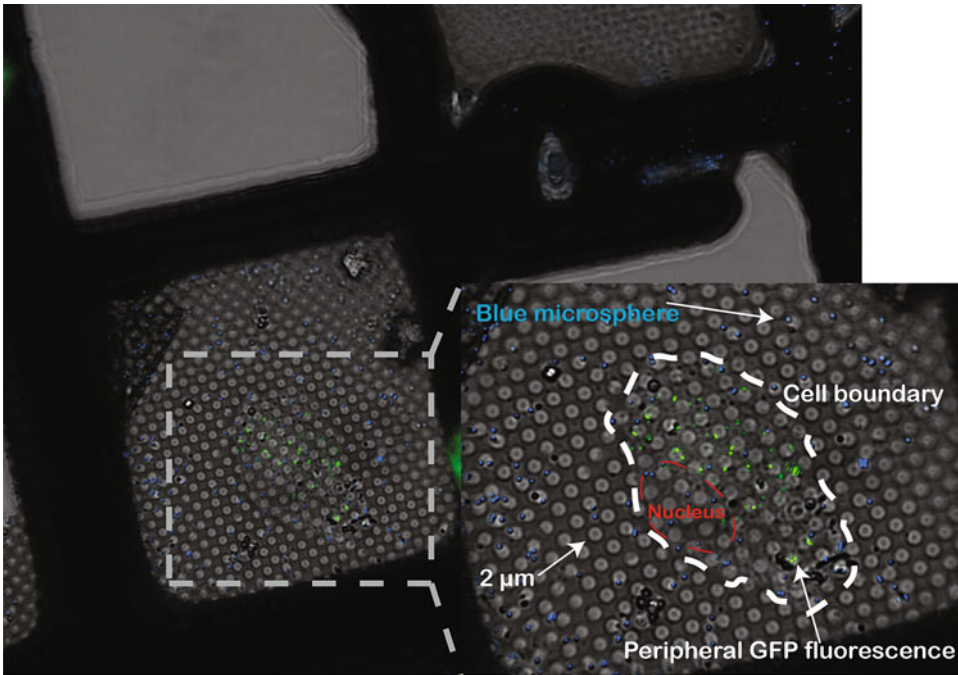


Fig. 1 Deconvolved cryo-LM image (composite of bright field and epifluorescence in FITC and DAPI channels) of U2OS cells, grown on London finder gold Quantifoil grids and stably expressing a GFP-tagged protein. Note the letter P which can be used for orientation. Relevant features are noted in the enlarged box

2.2.6 FIB-Milling for Imaging Thicker Regions of the Cell

In cryo-ET, sample thickness is a critical factor for data collection. Because of inelastic scattering, the application of cryo-ET is usually restricted to samples thinner than 600 nm, like small bacterial cells or the thin peripheral regions of eukaryotic cells. However, most regions of eukaryotic cells and many bacteria are thicker than that; thus, additional thinning procedures are required for cryo-ET to gain access to these samples (Fig. 2a). In recent years, cryo-FIB-milling has been developed as a tool to make thin lamellae from a thick sample while preserving most of the native state of the molecules. The concept of FIB-milling is to use high-energy ions such as gallium to remove materials above and below a targeted area. When milling at a low angle, this will create a lamella, usually a few hundred nanometers thick amenable for cryo-ET (Fig. 2b–d). Here, we describe how to do cryo-FIB-milling on an FEI Versa FIB/SEM equipped with a Quorum cryo-transfer system.

1. To prepare the Quorum transfer system for cryo work, mount the Quorum cryo-stage on the SEM stage.
2. Start the Quorum system in manual mode to pump vacuum in the chamber and scaffold. Prep-chamber vacuum should reach less than 6×10^{-6} before cooling to avoid contamination.

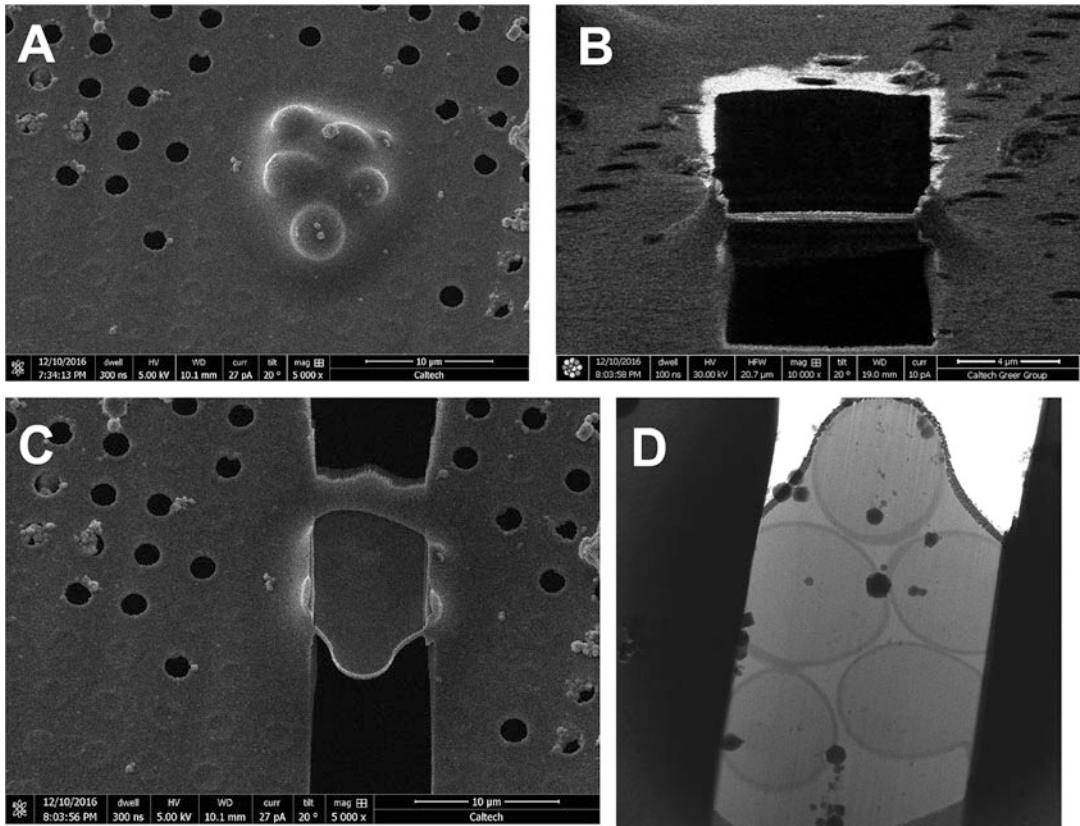


Fig. 2 Preparation of a lamella by focused ion beam milling. (a) SEM image (top view) of a cluster of yeast cells. (b) FIB image (oblique side view) of the lamella after milling and polishing both the top and bottom of the cell. (c) SEM image (top view) of the lamella at high magnification. (d) Lamella imaged by cryo-TEM

3. Pump the nitrogen gas isolated line to reach a vacuum lower than 5×10^{-2} mbar. This is important for the liquid nitrogen cooled gas to remain cold before it reaches the stage.
4. Set the temperature of the cryo-stage and anti-contaminator to desired number. Note that the temperature of the anti-contaminator is usually 20° lower than the stage. Set gas flow to auto. If using a self-pressured tank, make sure the pressure is higher than 30 psi.
5. Put the cooling rod into the liquid nitrogen dewar. Wait until the cryo-stage and anti-contaminator have reached their desired temperatures (usually -168°C and -188°C respectively). This usually takes 30–40 min.
6. To begin the sample transfer to the SEM cryo-stage, the shuttle and loading box should be pre-cooled with liquid nitrogen. Grids need to be clipped into autogrids with the cell side (the flat side) facing down before transfer to the loading box.

7. All tools used should be pre-cooled before contacting the sample.
8. Place the autogrids into the shuttle with the cell side facing up. Depending on which type of shuttle is used, you can load 1–2 autogrids at a time.
9. After attaching the transfer-unit's insertion rod to the shuttle, pump the vacuum in the slush chamber until liquid nitrogen freezes. Lift out the shuttle into the transfer unit and vent the slush chamber.
10. Attach the transfer unit to the airlock of the prep-chamber and press “pump vacuum.” The vacuum has to reach a certain level to safely open the airlock valves. A layer of platinum can be sputter-coated in the prep-chamber to increase conductivity and provide additional protection to the sample.
11. After the vacuum in the prep-chamber reaches the desired level, open the valve between the prep-chamber and SEM. Make sure the SEM cryo-stage is in the loading position. Transfer the shuttle onto the cryo-stage with the insertion rod and then retract the rod. The transfer unit should be removed and the valves should be closed.
12. To begin milling lamellae, the electron and ion beams should be in the operational state.
13. Move stage to image position and adjust focus and astigmatism for the electron beam. Link Z to FWD after doing so.
14. Find a marker on the grid and adjust eucentric height so the ion and electron beams point to the same location.
15. An additional layer of organometallic platinum can be deposited using the gas ingestion system (GIS) in the SEM. A detailed description of the operation of the GIS can be found in a protocol developed by the Baumeister lab [33].
16. The milling process usually starts with a higher current like 0.3 nA or 100 pA depending on the settings your FIB/SEM has. Two rectangular areas several microns in width (in mammalian cells, usually 10 μm) are drawn above and below the target region. Leave 3–5 μm in between to avoid damage by high-current ions.
17. Reduce the current to 30 pA and redraw the pattern of milling to remove any material left. Leave ~ 1 μm between the two patterns.
18. Use a current of 10 pA to do the final cleaning and reduce the thickness of the lamella to 200–500 nm. For this last step of milling, an additional 1° tilt can be added so the final thickness of the lamella is more homogenous.

19. Multiple places on the grid can be milled. When done, transfer the shuttle back to the transfer unit, and close the valve.
20. After venting the airlock, place the transfer unit on the slush chamber and pump. When the vacuum has reached 10^{-2} , open the valve on the transfer unit and place the sample in liquid nitrogen. All steps in this part should be performed gently to avoid any damage to the lamella. The slush chamber can be pre-pumped beforehand so it can reach the desired vacuum faster.
21. The sample can then be stored in clean liquid nitrogen for cryo-ET.

2.3 Biological (Plant) Tissues

The following will focus on plant tissues; however, the workflow of High Pressure Freezing (HPF)—cryosectioning—cryo-ET can be adapted to other types of tissues suitable for HPF. Preparation of plant tissues for HPF and cryosectioning are discussed in further detail in references [34, 35]. We will focus here on two plant tissues: in vitro grown 6-day-old root tips and PSB-D *Arabidopsis* Landsberg *erecta* cells grown in liquid medium.

2.3.1 Tissue Cultivation

1. Liquid cultured PSB-D cells are grown in Murashig and Skoog with Minimal Organics (MSMO, *Sigma-Aldrich*) with sucrose pH 5.7 with added Kinetin (*Sigma-Aldrich*) and 1-Naphthaleneacetic acid (NAA) (*Sigma-Aldrich*). Dispatch 75 mL of media in four 250 mL flasks (*Pyrex No 4980*) and cultivate at 25 °C, continuous illumination (20 $\mu\text{E}/\text{m}/\text{s}$) with 120 rpm shaking.
2. Seeds are sterilized in bleach. 100 mL of commercial bleach is placed in a beaker in a large plastic Tupperware, in a chemical fumehood (*see Note 12*). Open 1.5 mL Eppendorf tubes containing the seeds are placed in a tube rack inside the plastic Tupperware. 3 mL of 100% HCl are added and the Tupperware is closed and left for 3–4 h. After treatment, the Tupperware is opened, and tubes are closed before transferring to a sterile hood. The seeds are aired out in the sterile hood by opening the tubes for 30 min. The bleach-HCl mix can be left in the chemical fumehood to evaporate.
3. *Arabidopsis* seedlings are grown in Murashig and Skoog medium + vitamins (*Duchefa Biochemie*), with 2-(*N*-morpholino)-ethanesulfonic acid (MES) buffer (*Euromedex*) and 3.5 g of plant agar (*Duchefa Biochemie*), pH 5.8 in square plastic petri dishes (*VWR*).
4. Sterilized seeds are resuspended in autoclaved DI water, then pipetted in horizontal lines onto the plates. The plates are then set vertically in a greenhouse at 22 °C, on a long day photoperiod (16 h, 100 $\mu\text{E}/\text{m}/\text{s}$) for a week to produce young root tips.

2.3.2 High Pressure Freezing of Plant Tissues

The size of plant cells (ranging from 15 to 50 μm), their large aqueous vacuoles and their pecto-cellulosic cell wall make them challenging to cryo-preserve. Optimal vitrification of whole plant cells can only be achieved by HPF and the samples must be less than 200 μm thick. In practice, any plant sample that can fit in the freezer carriers used for HPF can be vitrified. However, experience shows that some freeze better than others. In general, the following materials are required for a HPF session of plant tissues:

1. Dextran cryoprotectant solution: 25% and 40% solutions are needed for the freezing of *Arabidopsis thaliana* root tips and cultured cells. 5 mL of each is sufficient.
2. Benchtop mini-centrifuge.
3. Dissection stereomicroscope.
4. Single edged carbon steel razor blades (*EMS*).
5. *X-Acto* knife set (for decapsulating tool) (*EMS*) or hemostatic forceps (*EMS*).
6. Tooth picks.
7. Various EM grade precision forceps (*EMS* style 2, 5, 5 \times , and Dumont style 7).
8. Freezing carriers: two types can be used for cryosectioning of plant tissues: the 200 μm deep brass carriers described in more detail elsewhere [35] or the 100 μm carriers composed of Type A gold-plated copper dishes (3 \times 0.50 mm with 0.1/0.2 mm cavities, *Technotrade International*) and Type B aluminum hats (3 \times 0.50 mm with a 0.3 mm cavity, *Technotrade International*).
9. Liquid nitrogen.
10. High Pressure Freezer: Bal-Tec HPM 010.
After preparing the above-mentioned materials, the process of HPF can be performed as follows:

2.3.3 Dissection and Freezing of Plant Tissues

1. Under a binocular loupe, put a drop of water on a glass slide.
2. Mount the bottom part of the type A carrier onto the Bal-tec HPM 010 freezing rod.
3. With a sharp razor blade, dissect the plant tissue of interest. The only requirement is that it is small enough to fit in the freezing planchette.
4. Quickly transfer the freshly dissected tissue to the type A carrier using the appropriate tools (forceps or toothpicks) and add a few μL of 25% Dextran until the liquid forms a shallow dome over the surface of the carrier.

2.3.4 Liquid Cultured Plant Cells

Cell pellets should be compact and dense. Hence, cells grown in liquid culture must be concentrated, usually by centrifugation before freezing. The sample should resemble a thick paste.

1. Spin down a 1.5 mL aliquot of the liquid culture using a tabletop centrifuge for 1 min at $1000 \times g$.
2. Discard the supernatant and resuspend in a small volume of 40% dextran.
3. Mount the bottom part of the brass carrier onto the Bal-tec HPM 010 freezing rod.
4. With a toothpick transfer the cells into the freezing carrier and add a drop of 40% dextran.

2.3.5 Sample Position Strategy

How the sample is positioned in the carrier will determine the cutting angle of the tissue (transversal or longitudinal) and can make the trimming process easier and more efficient.

Because each project and sample have their own requirements, here we will detail the advantages and disadvantages of two types of carriers used in our laboratory.

1. 200 μm brass carrier (used for PSB-D cell pellets)

In this system, the sample + cryoprotectant filler are laid in the bottom part of the carrier to form a prominent bubble, which is then enclosed by the concave top of the carrier (Fig. 3a). This system allows rapid trimming because the sample is more prominent; however, vitrification is only optimal in the edges of the sample, with the deeper parts usually forming hexagonal ice. This type of holder is appropriate for dense pellets of cells, where direction and area do not matter since the cells are randomly oriented in the pellet.

2. 100 μm type A gold-plated copper carrier (used for *Arabidopsis* root tips).

In this carrier, the sample + cryoprotectant filler forms a flat film within the rim of the carrier (Fig. 3b). This provides the advantage of homogenous vitrification throughout the thin sample. The disadvantage is that the carrier needs to be trimmed from the side until the sample is reached (Fig. 3b). This system is appropriate for tissues less than 100 μm thick that require sectioning in a particular orientation.

After positioning the sample in the desired way inside the carrier, place the lid of the carrier on top of the sample, and secure it on the freezing rod and subsequently put it into the slot of the Bal-tec HPM 010 and perform HPF. From this point on, the samples should never be taken out of liquid nitrogen.

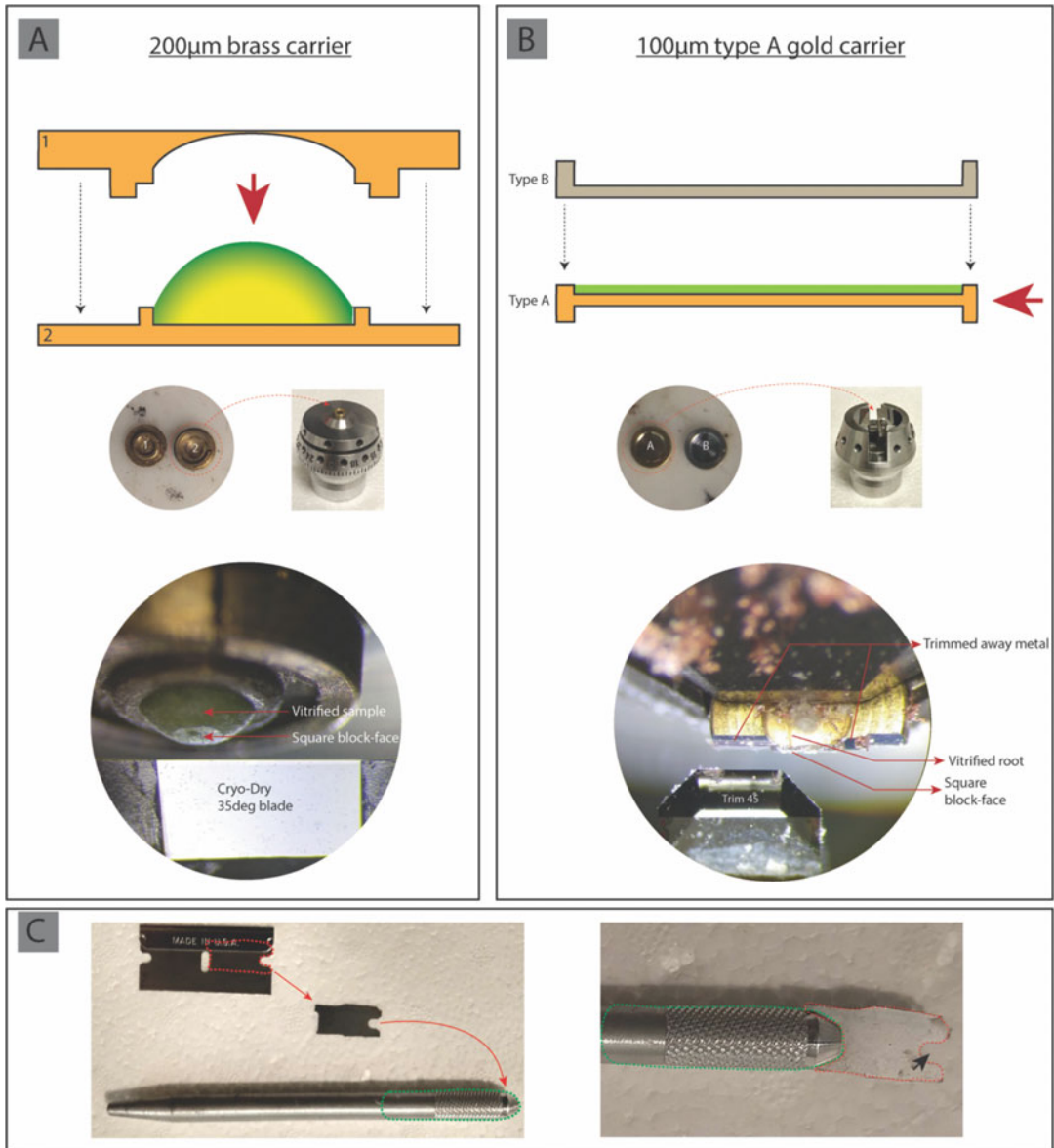


Fig. 3 (a) Top: schematic of a 200 µm brass carrier. Dashed arrows indicate how the system closes and red arrow indicates direction of sectioning. Green to yellow gradient indicates vitrification efficiency of sample (green = vitreous, yellow = hexagonal ice). Middle: top views of the carrier and its corresponding specimen holder. Half #2 lays flat in the specimen holder (dashed circle and arrow). Bottom: carrier containing a vitrified cell pellet mounted in the specimen holder in the cryo-ultramicrotome chamber facing the cryo-dry 35° knife. The block-face is visible on the cryo-planed surface. (b) Top: schematic of type A carrier. Dashed arrows indicate how the system closes and red arrow indicates direction of sectioning. Middle: top views of the type A and B halves and corresponding specimen holder. The carrier is mounted vertically in the clamp of the specimen holder (dashed circle and arrow). Bottom: trimming through the carrier to reach the sample. (c) Home-made decapsulating tool used to open the brass carriers after freezing. The screw tightening pen is outlined in green and the lever, carved from a razor blade in red. The groove where the carrier is placed is indicated by a black arrow

2.4 Cryosectioning of Plant Tissues

Cryosectioning consists of two steps: (a) trimming, where the block-face is carved out [35], and (b) cryosection collection in which the block-face is sectioned and the resulting sections and/or ribbons are collected on EM grids. The required material in order to perform cryosectioning followed by Cryo-Electron Microscopy of Frozen Hydrated Sections (CEMOVIS) has been previously addressed thoroughly [35, 36]. In general, the following materials are required for a cryosectioning session of plant tissues:

1. 200 mesh carbon-coated copper finder grids (*Ted Pella Inc*) or copper 200 mesh R2/2 NH2 Quantifoil grids.
2. Trimming knives: Trim 20 and Trim 45 (*Diatom*).
3. Section collection knives: Cryo-dry 25°, 35°, or 45° (*see Note 13*) (*Diatom*).
4. Hair (eyelash, blonde baby, or Dalmatian) glued to the tip of a wooden stick for cryosection manipulation.
5. Static line ionizer (*Diatom*).
6. Leica *Ultracut UCT* with *Leica EMFCS* cryo-chamber (*Leica Microsystems*) or equivalent cryo-ultramicrotome and associated microtools (pen-like pressing tool, freezing carrier holders, etc.).
7. Micromanipulator (for more stable ribbon collection).
8. Large amounts of liquid nitrogen.
9. Hair dryer or heating bench to warm and dry the tools.
10. Various EM grade precision forceps (EMS style 2, 5, 5×, and Dumont style 7).

After preparing the above-mentioned materials, the process of cryosectioning can be performed as follows:

2.4.1 Preparation

1. Cool down the cryo-ultramicrotome to $-165\text{ }^{\circ}\text{C}$ (*see Note 14*).
2. Mount the carrier in the cryo-ultramicrotome (*see Note 15*).
3. Decapsulate the lid of the carrier using a home-made tool (Fig. 3c).
4. Install and cool the knives, setting them as far as possible from the specimen holder to prevent accidental heat transfer.

2.4.2 Trimming

1. Light the system from below in order to highlight the knife-to-sample distance.
2. Bring the knife close to the sample, using the command panel and/or sliding the knife platform forward. Use the command panel only in the final stages of approach.

3. If the block has already been started, line up the knife with the cryo-planed surface by rotating the knife holder until the thin light sheet emerging below is of homogenous thickness.
4. Introduce the cryostat into the chamber and set to 25–30%.

2.4.3 *Trimming Domes from the 200 μm Carrier*

1. Manually advance the block for a few microns and then set it on automatic mode with a feed <100 nm and a cutting speed between 80 and 100 mm/s until reaching a depth of approximately 10 μm . The circular cryo-planed area should have a very smooth, reflective surface without any irregularities or holes. If not, vitrification is not good, and the sample should be discarded.
2. Cut 50–100 μm more on the left and right sides of the cryo-planed circle to generate a prominent thin vertical rectangle.
3. Rotate the specimen holder by 90° in order to make a square block-face.
4. Finish block-face by repeating **step 2** above.

2.4.4 *Trimming the Type a 100 μm Deep Carrier*

This method entails cutting through metal and sample, two materials with different cutting properties. Trimming steps should favor as much as possible cutting through only one material at a time. When cutting through both cannot be avoided, the cutting speed should be reduced.

1. Orient the specimen holder so that the carrier is presented vertically to the knife.
2. Bring the knife to the carrier.
3. Trim through the metal at 70 nm feed and 60–80 mm/s speed. It will take approximately 800 μm of trimming to reach the sample.
4. When the sample is reached, reduce the trimming speed to 50 mm/s. At this point, you will be cutting through the dextran and the sample will look like a clear circular structure.
5. Continue cutting until the sample enlarges horizontally to fill the full 100 μm depth of the carrier. At this point, there should be a vertical separation between the sample and the bottom of the carrier.
6. Shift the knife in order to cut only through the vertical metal and not the sample.
7. Trim 200 μm deep, gradually approaching the sample at 100 mm/s (*see Note 16*).
8. When both the sample and metal are being trimmed, lower the speed to 50 mm/s.
9. When the vertically oriented sample is well cleared on both sides, rotate 90°.

10. Trim the metal on both sides at 100 mm/s to a depth of 200 μm .
11. Trim through the frozen dextran on each side in stages, each approximately one-fourth of the width of the diamond blade, until the final width of the block-face is reached.

The section collection technique is precisely described in reference [35] and thus will not be repeated here. The nominal cryosection thickness should be around 100 nm for tomography.

2.5 Other Samples

These include any purified organelle, compartment [37], in vitro assembly [38], or purified protein complex. The sample should be purified and concentrated as gently as possible to avoid damage [28, 39]. As many of these samples are thin, they can be suitable for high-resolution tomography. These samples are compatible with the different material sections discussed above. However, for high-resolution samples, we typically use Protochip C-flat 2/2 holey carbon grids with 300 mesh, and mix the sample with 10 nm gold fiducials.

3 Data Collection

A detailed protocol for data collection and processing is available in reference [40].

3.1 Data Acquisition Using SerialEM: Conventional Tilt-Series

After loading the samples to the microscope (in our lab a Titan Krios) and assuming that the microscope is already aligned, data collection can be started. Currently, we use SerialEM [41] to collect our data. We refer the reader to the tutorial of SerialEM for detailed discussion of what the software can do. In general, we start by making an atlas of the grid at low magnification ($82\times$). This will give a general idea of how the grid looks and the ice gradient. Subsequently, a montage of some good squares (at magnification $2245\times$) is collected providing a better view of the cells on these squares. Subsequently, points are added on cells in the holes (or other interesting cells in the montage). Then, the stage is moved to each of these points and a preview image (with low dose) is taken for that cell. The position of the cell is optimized, for instance, centered or offset if one wants to collect data from a pole of the cell). After that, a view image (at medium magnification, $2245\times$) is taken and is saved and used as the anchor state. View images are used to help tracking and aligning the target during data collection. One can further proceed with the process for all the required targets by pressing the “Anchor map” button. At the end, click the “TS” (tilt-series) option for the targets where data will be collected and tilt-series parameters are filled in as required (e.g., starting and ending angles, increment degrees, defocus, how to change exposure time with tilting angle). Once that is done, click

on “Navigator” in the main menu and go to “Acquire at points”, where data collection can be started. Usually, we select “Rough eucentricity”, “Autofocus”, and “Autocenter beam” for batch collection. To calculate the exposure time, we use the following equation:

$$\text{Exposure time (s)} = \left[\text{Total Dose (e}^-/\text{\AA}^2) \times (\text{Pixel size (}\text{\AA}\text{)})^2 \right] / [(\text{Dose measured e}^-/\text{pix/s}) \times (\text{Number of images in the tilt - series})]$$

where

Total dose is the total dose desired, usually between 100 and 200 e⁻/Å².

Pixel size depends on the magnification used to collect data.

Dose measured is the number of electrons (e⁻/pix/s) passing through the hole. For K3 cameras, this can be up to 30 e⁻/pix/s on the sample area.

Number of tilt images in the tilt-series depends on the maximum and minimum tilt angles and the angular increment (e.g., a tilt-series from -50° to +50° with 1° step will have 101 images).

3.2 Rapid Tilt-Series Acquisition

Two rapid tilt-series methods are currently being developed on a Titan Krios (Thermo Fisher Scientific) equipped with a single-axis holder: continuous-tilting and fast-incremental [31]. In continuous-tilting, the camera continuously records frames as the sample is tilted. For this reason, only unidirectional and bidirectional tilt-schemes are possible. In fast-incremental, even though the camera also records continuously, the beam shutter is used to rapidly expose the target at discrete tilt angles, resulting in blank frames while the stage is tilting, and allowing more complex tilt-schemes, such as dose symmetric [14]. Figure 4 shows examples of cellular features reserved in tomograms collected using both methods.

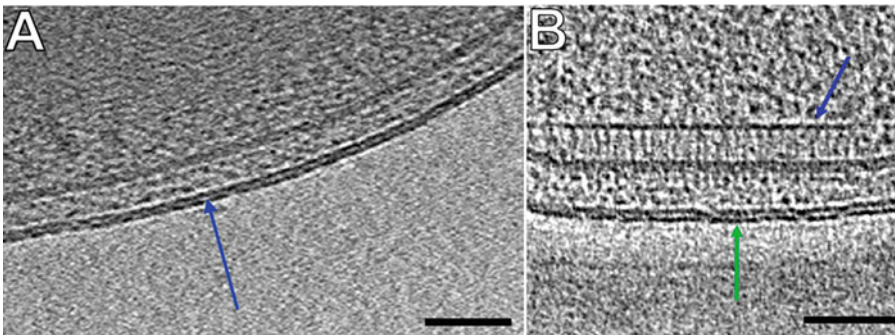


Fig. 4 Snapshots taken from tomograms acquired using the (a) continuous-tilting, and (b) fast-incremental methods display visible features. (a) The double leaflet of the outer membrane lipid bilayer (blue arrow). (b) Side view of a chemoreceptor array (blue arrow), and the outer membrane lipid bilayer (green arrow). Figure adapted from Ref. 31

3.2.1 *Pre-data Collection Steps*

Because the target is not tracked during tilting, both methods require accurate eucentric height measurement prior to collecting data to minimize field-of-view loss. While this is currently being optimized, we describe one method to measure eucentric height below.

1. Find and center the desired target in the field of view at “Record” magnification in low-dose mode.
2. Perform a rough eucentricity adjustment routine to adjust the Z-height to the eucentric point by clicking the “Eucentric-Rough” command in the Tasks menu.
3. Run the “Realign to item” command to recenter the target in the field of view after rough eucentricity.
4. Perform the fine eucentricity routine in the Trial area, at the same magnification as data collection. First, check the “Use Trial in LD Refine” command in the Tasks menu, then click the “Eucentric-Fine” command. Ensure the Trial area is unobstructed.

3.2.2 *Continuous Tilting Data Collection in SerialEM*

For a unidirectional tilt-scheme, from -60° to $+60^\circ$:

1. Set the exposure time in the Record settings to be long enough to record the entire tilt-series.
2. Turn on dose fractionation and select an adequate time per frame.
3. Tilt to -60° .
4. Run the command “TiltDuringRecord #A #D” to record while tilting the stage to angle #A after a delay of #D in milliseconds. For instance, TiltDuringRecord 60 1000.

For a bidirectional tilt-scheme, starting from 0° :

5. Set the exposure time in the Record settings to be long enough to record each direction of the tilt-series.
6. Turn on dose fractionation and select an adequate time per frame.
7. Tilt to 0° .
8. Run the command TiltDuringRecord -60 1000.
9. Return to 0° .
10. Run the command TiltDuringRecord 60 1000.

3.2.3 *Fast-Incremental Data Collection in SerialEM*

SerialEM version 3.7 includes the FrameSeriesFromVar command, which allows the collection of fast-incremental data given an input array variable that describes each step of the tilt-scheme.

1. Generate the array variable containing the following information for each tilt, separated by spaces: Tilt Angle, Shutter open time (exposure time), Wait time between step (before opening

the shutter), change in defocus, image shift in X, image shift in Y. Units for the last three entries are all in microns. By saving the array as a persistent variable in SerialEM, this step only needs to be done once per tilt-scheme.

2. A typical fast-incremental SerialEM script includes the following commands:
 - (a) “FrameThresholdNextShot 0.1” automatically skips saving blank frames based on a mean value below a threshold of 0.1. This threshold can be adjusted as desired.
 - (b) “FrameSeriesFromVar var 31 #d”, where #d is an initial delay time, followed by the Record command to record movie frames.
 - (c) ReportLastFrameFile, to assign the filename to reported Value1.
 - (d) “WriteFrameSeriesAngles \$reportedValue1.angles” writes the tilt angles collected into a text file appended with .angles for post-processing.

3.3 Data Collection for High-Resolution (Near-Atomic) Tomography

Data collection for high-resolution tomography begins with determining the desired resolution, and choosing parameters based on both the desired resolution and the features of the object of interest. Collection is typically optimized through one or more sessions, with alignment and subtomogram averaging resolution used to determine optimal settings.

For higher-resolution collection, samples must be thin (ideally less than 200 nm) and fiducials must be plentiful (typically 20 or more beads in the field of view). The data collection is typically reminiscent of a single-particle averaging collection, with a pixel size of less than 2 Å, defocus gradient of -1 to -5 μm , and dose-fractionated frame collection [28, 42]. If subtomogram averaging is intended, a phase plate is not recommended. The tilt-scheme begins at zero degrees and is acquired with symmetric dose alternating between positive and negative angles [28]. Optimal dose is determined based on the point at which the sample displays visible damage, but is often approximated at 120 electrons/Å² with the highest accumulated doses at the highest tilt angles. Tilt increment and dose have frequently been set to -60° to $+60^\circ$ in 3° increments, but smaller tilt increments or a larger range may be beneficial for some samples.

Also, particular attention is paid to minimize the dose used to find and center the target and for setting the eucentric height and to minimize drift during exposure. Movies can be collected to motion-correct any residual drift. In addition, it is recommended to use off-targets focus spots to maintain focus throughout tilt-series collection. Finally, the beam has to be highly coherent and parallel to preserve high-resolution signals.

3.4 Imaging Fluorescent Targets in the Titan Krios Using Cryo-CLEM

1. Use SerialEM to collect a 200 \times magnification montage for each EM grid loaded into the Titan Krios (*see Note 17*).
2. Find a cell of interest imaged previously by cryo-LM using the letters, symbols, or numbers of the grid support.
3. Use the whole-grid 200 \times montage to generate a polygon montage of the thin cellular peripheral area of interest and surrounding area. It is advisable to capture fluorescent microspheres in the surrounding area in this montage for registration of the EM and LM images (*see Note 18*).
4. Using your polygonal montage, evaluate if the ice is too thick for tilt-series collection by evaluating the hole that is closest to the fluorescent puncta using the cryo-LM aligned phase contrast/fluorescence images for orientation.
5. If the ice is thin enough, overlay the fluorescence images with the polygonal montage images using the fluorescent microspheres seen in both the LM and EM modalities. Any image processing software can be used to roughly align the images.
6. Next, localize more precisely the location of the fluorescent puncta in the thin edge.
7. Collect a tilt-series in this location.

4 Data Processing and Tomographic Reconstruction

4.1 Conventional Tilt-Series

We reconstruct tomograms from raw tilt-series using the IMOD software [41, 43, 44]. We refer the reader to the useful IMOD tutorial (<http://bio3d.colorado.edu/imod/doc/tomoguide.html>). We also refer the reader to our recently published chapter [32] where a similar procedure is described for bacterial secretion systems.

The tilt-series is opened (“Build Tomogram”) using the IMOD program Etomo’s graphical user interface (GUI). Fill the diameter of the gold fiducials and specify the tilt-series axis type. Click “Scan header” to scan the pixel size and image rotation. Then, click “Create Computer Scripts”. Following this, several steps will appear on the GUI that need to be performed. These steps include:

4.1.1 Pre-processing

During this step, pixels with very high or low values are removed using “Ccderaser” to circumvent the generation of artifacts. Use value 10 for “Peak criterion” and 8 for “Difference criterion”. Generate a stack by clicking “Create Fixed Stack”, then check the quality of the stack by clicking “View Fixed Stack” and remove any bad images from the stack then click “Use Fixed Stack”.

- 4.1.2 Coarse Alignment** The aim of this step is to align the images of the tilt-series using cross-correlation before producing a finer-aligned stack using the fiducials. Click first “Calculate Cross-Correlation” and then “Generate Coarse Aligned Stack.” Check the aligned stack by clicking “View Aligned Stack in 3dmod.” Remove any bad images from the stack and create and use a new stack lacking the bad images.
- 4.1.3 Fiducial Model Generation** If the sample has gold fiducials, these can be tracked, usually using the “Make seed and track” or “Raptor” option. Generally, we select between 10 and 30 beads. We usually begin with “Make seed and track”, activate the “Refine center with Sobel filter” provide a value of 8, and then click “Generate Seed Model” in the “Track beads” subwindow. After that, click “Fix Fiducial Model” to fix any untracked or badly tracked beads manually. If the tracking using “Make seed and track” is bad, one can try tracking the beads using “Raptor”. Tracking with “Patch Tracking” is usually used for eukaryotic samples which lack gold beads in many cases.
- 4.1.4 Fine Alignment** Click “Compute Alignment” to correct the inappropriately placed fiducials by clicking “View/Edit Fiducial Model.”
- 4.1.5 Tomogram Positioning** A tomogram thickness value is provided (usually a thickness of 600 is used for many single-small-cell samples). Click “Create Whole Tomogram” with a binning of three and after that “Create Boundary Model”. Rotate the tomogram 90°, save the model, and click on “Create Final Alignment”.
- 4.1.6 Final Aligned Stack** Here, we only perform “Create Full Aligned Stack”. However, one can also apply “Contrast Transfer Function (CTF) correction”, “Erase Gold”, and/or “2D Filter”.
- 4.1.7 Tomogram Generation** The aligned image stack is used to build the tomogram by using either: (a) Weighted Back Projection or (b) Simultaneous Iterative Reconstruction Technique (SIRT-like). The generated tomogram can be viewed by clicking “View Tomogram in 3dmod.”
- 4.2 Fiducial-Less Patch Tracking Using IMOD** Sometimes it is difficult to add gold fiducial markers to a specimen, particularly FIB-milled lamellae or cryosections. In these cases, the alignment is usually done by image correlation within. Here, we briefly describe how to reconstruct data without fiducials by using the patch tracking method in IMOD. More detailed information can be found on the IMOD website: <https://bio3d.colorado.edu/imod/doc/patchTrackExample.html>
1. Raw tilt-series are usually dose-weighted to boost the contrast of higher angle tilt images.
 2. Data are imported and pre-processed in IMOD as described before.

3. In the “Fiducial Model Generation” step, select “Use patch tracking to make fiducial model.”
4. Change the patch size, for cryo-tomograms a larger patch size is recommended. Note that you can use the “Use boundary mode” option to only patch-track a subarea of the tile-series. This is often used to avoid areas with few features or with contamination.
5. The “Advanced” button at the bottom gives options to play with filter parameters, trimming pixels and range of views, etc.
6. Check “Break contours into pieces” to perform robust fitting with a tuning factor.
7. Click “Track Patches.”
8. After this is done, go to “Fine Alignment.” Make sure to check “Do robust fitting with tuning factor” and turn on “Find weights for contours, not point”. Click “Compute Alignment.” This will give you a mean residual in the log window.
9. Press “View/Edit Fiducial Model.” All the tracks will be shown with overlapping segments. Tracks with obvious mistracking can be deleted. If needed, go back to **step 4** above to refine the region used for tracking until you reach the desired alignment quality.

4.3 Rapid Tilt-Series Processing

4.3.1 Continuous tilting data

Due to low signal-to-noise ratio (SNR) of individual images, some processing is required to enhance the contrast for fiducial tracking. One strategy we use is to sum neighboring images to enhance the contrast of fiducials at each tilt angle (Fig. 5). This requires neighboring images to first be stretched by an amount equal to the cosines of its tilt angle and of the tilt angle of the reference image, followed by motion correction. These functions have been coded in the Neighbor-enhance script, which requires the IMOD package.

1. Download the Neighbor-enhance script and the accompanying rotmagstr program (<https://github.com/chreifi/fasttilt>) and add both to your list of environment variables on your linux machine.
2. Run the Neighbor-enhance script to gain normalize, correct defects, remove deviant pixels, stretch, align, and sum images, and perform a rough alignment of each summed image of the tilt-series. Outputs are the raw data after gain normalization, defect correction, and deviant pixel removal (.st), a roughly aligned contrast-enhanced tilt-series (.preali file) and the transforms (.xf, .xg).
3. Run the eTomo software in the IMOD package, using the raw tilt-series as input. Enter values for the tilt axis angle, start angle, and an estimate of tilt increment.

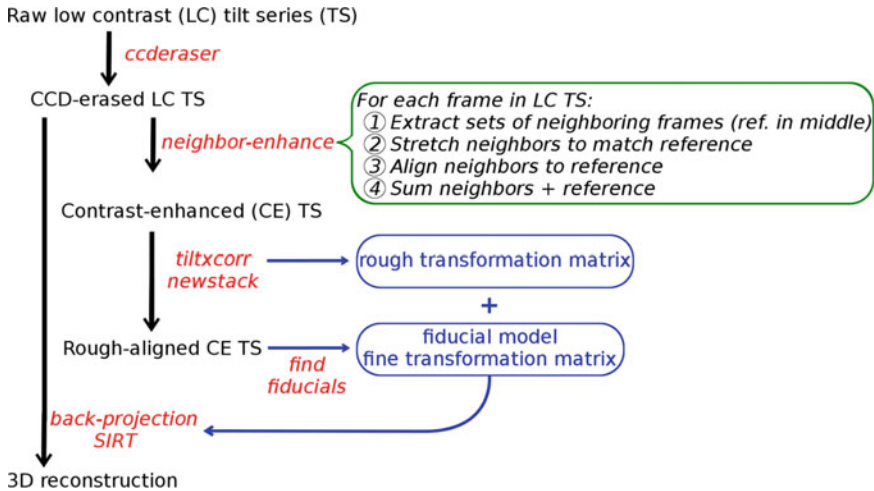


Fig. 5 Workflow for processing data acquired using the continuous-tilting method. Font color is black for tilt-series data, red for programs and scripts, and blue for alignment transforms. A general description of the Neighbor-enhance script is shown in the green box. Figure adapted from Ref. 31

4. Skip directly to seed model creation to generate a seed model and track the beads throughout the tilt-series. These steps are identical to conventional tilt-series alignment.
5. Using IMOD, the transforms generated by the fiducial model will automatically be applied to the raw tilt-series (original input). The reconstruction step is thus also identical to conventional tilt-series as shown below.

4.3.2

Fast-Incremental Data

The current SerialEM version (3.7) produces a single stack of movie frames containing the entire tilt-scheme data and skips saving blank frames based on a user-defined threshold. Nevertheless, the program automatically pads the tilt-series with one blank frame at the start, and one at the end, which first need to be removed. Frames that are part of each discrete tilt angle must then be extracted, motion-corrected, and placed into the final tilt stack in the correct order. We have written a bash script that performs these post-processing steps.

1. Download the Fast-incremental script (<https://github.com/chreifi/fasttilt>) and add it to your list of environment variables on your linux machine.
2. Execute the script, providing the following files for input: input tilt-series, angles.txt file obtained from running the WriteFrameSeriesAngles function in SerialEM, as well as gain reference and defects file. The script also provides options for doing motion correction using Alignframes or Motioncor2.
3. Once successfully processed, the output tilt stack from the Fast-incremental script can be processed in IMOD just as in conventional cryo-ET.

4.4 Data Processing for High-Resolution Tomography

Data processing for high-resolution tomography mirrors that of conventional data processing, but with additional steps to optimize data. Recently, user-friendly software packages have been developed (EMAN2, emClarity, relion); however, to date every novel high-resolution subtomogram averaging structure has been based on a workflow utilizing multiple software packages and personal scripts [27, 28, 38, 42].

1. Frame alignment: gain-correct, rotate, and align the tilt frames in the software of your choice. IMOD alignframes or MotionCor2 both perform well for frame alignment.
2. Dose-weighting: tilts should be dose-weighted prior to tilt stack alignment. All available software methods are based on the single-particle averaging estimation of the relationship between electron dose and final resolution from the Grigorieff group [45].
3. CTF estimation: the CTF can be estimated with any standard software package. However, CTF estimation software routinely underperforms at high tilt angles. It is common to test multiple packages for different data collections or to use homemade software to assess or improve outputs.
4. Reconstruction: the most common reconstruction method is weighted back projection, coupled with either two-dimensional CTF correction in IMOD or three-dimensional CTF correction in NovaCTF [46]. For low-defocus tomograms, an SIRT-like filter can be applied during reconstruction for visualization purposes.
5. Subtomogram averaging: for a low particle count (100s), high resolution is not expected and PEET or RELION may be used as in conventional tomography. For particle counts above 10,000, high-resolution subtomogram averaging often involves parallelized GPU processing and a highly sample-specific workflow. Dynamo and AV3 have both performed to high resolution on novel structures [28, 42] and are flexible for a customized workflow. emClarity and EMAN2 have performed to high resolution on a dataset previously solved in AV3, but are less flexible for advanced users.

4.5 Subtomogram Averaging

In subtomogram averaging, certain subvolumes are cropped from the tomogram, aligned, and then averaged to enhance the signal-to-noise ratio of a certain repetitive feature (e.g., a protein complex of interest) within a single tomogram or across different tomograms of the same species collected with similar pixel size. Many software packages are currently available to perform subtomogram averaging, including: Dynamo, PEET, RELION, EMAN2, and PyTOM (*see, e.g., Refs. 47–52*).

As an example, we will discuss how to perform subtomogram averaging using PEET, a routine procedure we do in our group. Open the tomogram using the command `3dmod` and activate the “Toggle between regular and high-resolution image” and “keep current image or model point centered” buttons. Activate the “Model” mode in the `3dmod` window and set the slicer thickness to ten and then go to “Edit” and select “Angles”. A new window will appear where the coordinates of each one of the chosen particles can be viewed. Find the optimal view of the complex of interest by rotating the particle and moving through the different slices of the tomogram and then save these coordinates and angles. Create a model point for each particle with a middle mouse click and then save this model.

Before averaging, compute an initial motive list (MOTL) by running the command “`stalkInit name.mod.`” Usually, we create a separate folder for the PEET run and then subfolders entitled “run1”, “run2”, etc. In “run1”, load all the tomograms, the MTOL files, and the “.slt” files (which have the tilt angles required for missing wedge compensation). In the first run, use one of the good particles as a reference without a mask. Subsequently, use the obtained structure from each run as a reference for the next run. Different masks can be constructed in IMOD to perform focused alignment on different parts of the protein complex. This process is repeated until the structure cannot be improved anymore. If the symmetry of the complex is known, this symmetry can be imposed on the structure; however, one should bear in mind that different parts of the complex might have different symmetries and imposing one specific symmetry might affect other parts of the complex that have different symmetries. If the symmetry is unknown, we usually apply two-fold symmetry along the mirror plane to improve the signal-to-noise of the side view (checking that no new densities appear compared to the non-symmetrized structure). Note that when two-fold symmetry is applied to a complex with unknown symmetry, no conclusions should be made on the top view of that average.

5 Notes

1. The use of phenol red-free media is advised to prevent the generation of unwanted autofluorescence at 80 K when imaging the cells using cryo-LM [53].
2. Over-digestion with trypsin may prevent the cells from adequately attaching and spreading on the grid.
3. Different types of films (silicon vs. carbon) and shapes of grids support (square vs. hexagonal) are available. For U2OS cells,

R2/2 square supports coated with Quantifoil holey carbon film are recommended. The R2/2 square support allows a sufficient area for the cells to adequately attach and spread on the grid.

4. To prevent the grid from sliding on the glass slide, both sides of the grid are coated with collagen.
5. We recommend touching the grid to the edge of the glass slide to gain optimal purchase.
6. Due to their increased contrast in low signal:noise tomograms of mammalian cells, 20 nm gold beads are used as fiducial markers to align the tilt-series. If performing cryo-CLEM, fluorescent microspheres are mixed and vortexed in 1:1 dilution with the 20 nm gold beads before being added to the grid. It is recommended that the gold beads be concentrated as much possible to ensure their presence around the thin edges of cells.
7. The grid is blotted from the side where the cells are not attached so as to prevent damaging the cells during the blotting process. Blotting is achieved by using a strip of blotting paper which has been folded 90° at its tip and held by tweezers which enter the Vitrobot chamber from the side port.
8. A liquid ethane/propane mixture is used to avoid solidification as when using ethane alone.
9. In our experience, the signal from GFP can be too weak to detect due to high background autofluorescence in cryogenic conditions. Using the brighter mNeonGreen fluorescent protein is recommended.
10. Collection of phase contrast and red, green, and blue fluorescence images is needed to distinguish autofluorescence from real fluorescent protein signal [53]. For example, in U2OS cells the blue channel can be used to distinguish the 0.5 µm Tetra-Speck Microspheres (which fluoresce bright red, green and blue, and are seen by phase contrast) from autofluorescence (bright red and green, dim blue), and real green fluorescent protein signal (bright green). We recommend plotting the intensities of puncta in the red, green, and blue channels in unlabeled cells vs. cells expressing the fluorescent protein to identify targets.
11. Aligning the fluorescent images to the fluorescent microspheres seen in the phase contrast image can help identify whether the target fluorescent protein signal is present in an area of the ice that has sufficient electron transparency.
12. Mixing HCl and bleach creates very hazardous chlorine gas therefore this should be done in a chemical fumehood with an exhaust leading to the exterior of the building rather than a hood which recycles air in the same room.

13. The lesser the angle of the knife, the less compression artifacts (crevassing) will occur on the cryosections, and the more fragile the blade will be. While a 25° cryo-dry knife will give the best results, it should be reserved for experts as it is fragile. The 35° knife is a good compromise between sturdiness and compression artifacts.
14. The devitrification temperature of water is −135 °C. Above this temperature, the sample will devitrify and cubic ice will nucleate and spread. The state of the ice in cryosections can be checked by cryo-electron diffraction.
15. For the cutting to be smooth, everything in the chamber needs to be tightened in order to eliminate sources of vibration during the process.
16. In order to optimize trimming time, it is good to trim as much metal as possible during the first trimming session. This way, when the sample block-face needs to be cleared after several section collection sessions, one will only need to trim 50 μm around the existing block-face, instead of going through the whole process again.
17. For high-resolution imaging and to prevent premature radiation damage, we recommend that each image of the montage be collected at a low-dose (0.5 e[−]/Å²) and far from focus (−40 μm) to maintain good contrast of the outline and thin edges of the cells.
18. Before collecting the polygon montage, align the whole-grid 200 × montage with the microscope X and Y stage coordinates using the “shift to marker” function in SerialEM.

Acknowledgments

Cryo-ET work in the Jensen lab is supported by NIH grants R35 GM122588, RO1 A127401, and P50 AI150464 and by the Howard Hughes Medical Institute and performed in the Beckman Institute Resource Center for Transmission Electron Microscopy. M.K. acknowledges a Rubicon postdoctoral fellowship from De Nederlandse Organisatie voor Wetenschappelijk Onderzoek (NWO). We thank Catherine M Oikonomou for reading and editing the manuscript.

References

1. Sigal YM, Zhou R, Zhuang X (2018) Visualizing and discovering cellular structures with super-resolution microscopy. *Science* 361:880–887
2. Hänsel R, Luh LM, Corbeski I, Trantirek L, Dötsch V (2014) In-cell NMR and EPR spectroscopy of biomacromolecules. *Angew Chem Int Ed* 53:10300–10314
3. Kaplan M et al (2015) Probing a cell-embedded megadalton protein complex by DNP-supported solid-state NMR. *Nat Methods* 12:649–652

4. Kaplan M et al (2016) EGFR dynamics change during activation in native membranes as revealed by NMR. *Cell* 167:1241–1251.e11
5. Oikonomou CM, Jensen GJ (2017) A new view into prokaryotic cell biology from electron cryotomography. *Nat Rev Microbiol* 15:128
6. Lučić V, Rigort A, Baumeister W (2013) Cryo-electron tomography: the challenge of doing structural biology in situ. *J Cell Biol* 202:407–419
7. Chang Y-W et al (2016) Architecture of the type IVa pilus machine. *Science* 351:aad2001
8. Kaplan M et al (2019) The presence and absence of periplasmic rings in bacterial flagellar motors correlates with stator type. *elife* 8:e43487
9. Chaban B, Coleman I, Beeby M (2018) Evolution of higher torque in campylobacter-type bacterial flagellar motors. *Sci Rep* 8:97
10. Kaplan M et al (2019) In situ imaging of the bacterial flagellar motor disassembly and assembly processes. *EMBO J* 38:e100957. <https://doi.org/10.15252/emboj.2018100957>
11. Ferreira JL et al (2019) γ -proteobacteria eject their polar flagella under nutrient depletion, retaining flagellar motor relic structures. *PLoS Biol* 17:e3000165. <https://doi.org/10.1101/367458>
12. Zhu S et al (2019) In situ structures of polar and lateral flagella revealed by Cryo-Electron tomography. *J Bacteriol* 201:13
13. Zhao X et al (2013) Cryoelectron tomography reveals the sequential assembly of bacterial flagella in *Borrelia burgdorferi*. *Proc Natl Acad Sci* 110:14390–14395
14. Hagen WJH, Wan W, Briggs JAG (2017) Implementation of a cryo-electron tomography tilt-scheme optimized for high resolution subtomogram averaging. *J Struct Biol* 197:191–198
15. Briggs JAG (2013) Structural biology in situ—the potential of subtomogram averaging. *Curr Opin Struct Biol* 23:261–267
16. Leigh KE et al (2019) Subtomogram averaging from cryo-electron tomograms. *Methods Cell Biol* 152:217–259
17. Murphy GE, Leadbetter JR, Jensen GJ (2006) In situ structure of the complete *Treponema primitia* flagellar motor. *Nature* 442:1062–1064
18. Chen S et al (2011) Structural diversity of bacterial flagellar motors: structural diversity of bacterial flagellar motors. *EMBO J* 30:2972–2981
19. Zhao X, Norris SJ, Liu J (2014) Molecular architecture of the bacterial flagellar motor in cells. *Biochemistry* 53:4323–4333
20. Gold VA, Salzer R, Averhoff B, Kühlbrandt W (2015) Structure of a type IV pilus machinery in the open and closed state. *elife* 4:e07380
21. Hu B, Lara-Tejero M, Kong Q, Galán JE, Liu J (2017) In situ molecular architecture of the salmonella type III secretion machine. *Cell* 168:1065–1074.e10
22. Ghosal D, Chang Y-W, Jeong KC, Vogel JP, Jensen GJ (2017) In situ structure of the legionella dot/Icm type IV secretion system by electron cryotomography. *EMBO Rep* 18:726–732
23. Chang Y-W, Shaffer CL, Rettberg LA, Ghosal D, Jensen GJ (2018) In vivo structures of the helicobacter pylori cag type IV secretion system. *Cell Rep* 23:673–681
24. Ghosal D et al (2019) Molecular architecture, polar targeting and biogenesis of the legionella Dot/Icm T4SS. *Nat Microbiol* 4:1173–1182
25. Yang W et al (2019) In situ conformational changes of the *Escherichia coli* serine chemoreceptor in different signaling states. *MBio* 10:e00973-19
26. Rapisarda C et al (2019) *In situ* and high-resolution cryo-EM structure of a bacterial type VI secretion system membrane complex. *EMBO J* 38:e100886
27. Wan W et al (2017) Structure and assembly of the Ebola virus nucleocapsid. *Nature* 551:394–397
28. Schur FKM et al (2016) An atomic model of HIV-1 capsid-SP1 reveals structures regulating assembly and maturation. *Science* 353:506–508
29. Rigort A et al (2012) Focused ion beam micro-machining of eukaryotic cells for cryoelectron tomography. *Proc Natl Acad Sci* 109:4449–4454
30. Danev R, Buijsse B, Khoshouei M, Plitzko JM, Baumeister W (2014) Volta potential phase plate for in-focus phase contrast transmission electron microscopy. *Proc Natl Acad Sci U S A* 111:15635–15640
31. Chreifi G, Chen S, Metskas LA, Kaplan M, Jensen GJ (2019) Rapid tilt-series acquisition for electron cryotomography. *J Struct Biol* 205:163–169
32. Ghosal D, Kaplan M, Chang Y-W, Jensen GJ (2019) In situ imaging and structure determination of bacterial toxin delivery systems using electron cryotomography. In: Buchrieser C, Hilbi H (eds) *Legionella*, vol 1921. Springer, New York, pp 249–265

33. Schaffer M et al (2015) Cryo-focused ion beam sample preparation for imaging vitreous cells by cryo-electron tomography. *Bio Protoc* 5:e1575
34. Nicolas W, Bayer E, Brocard L (2018) Electron tomography to study the three-dimensional structure of plasmodesmata in plant tissues—from high pressure freezing preparation to ultrathin section collection. *Bio Protoc* 7:1
35. Ladinsky MS (2010) Micromanipulator-assisted vitreous cryosectioning and sample preparation by high-pressure freezing. *Methods Enzymol* 481:165–194
36. Ladinsky MS, Pierson JM, McIntosh JR (2006) Vitreous cryo-sectioning of cells facilitated by a micromanipulator. *J Microsc* 224:129–134
37. Iancu CV et al (2007) The structure of isolated *Synechococcus* strain WH8102 carboxysomes as revealed by electron cryotomography. *J Mol Biol* 372:764–773
38. Kovtun O et al (2018) Structure of the membrane-assembled retromer coat determined by cryo-electron tomography. *Nature* 561:561–564
39. Metskas LA, Briggs JAG (2019) Fluorescence-based detection of membrane fusion state on a cryo-EM grid using correlated cryo-fluorescence and cryo-electron microscopy. *Microsc Microanal* 25:942–949
40. Resch GP (2019) Software for automated acquisition of electron tomography tilt series. *Methods Cell Biol* 152:135–178
41. Mastronarde DN (2005) Automated electron microscope tomography using robust prediction of specimen movements. *J Struct Biol* 152:36–51
42. Hutchings J, Stancheva V, Miller EA, Zanetti G (2018) Subtomogram averaging of COPII assemblies reveals how coat organization dictates membrane shape. *Nat Commun* 9:4154
43. Kremer JR, Mastronarde DN, McIntosh JR (1996) Computer visualization of three-dimensional image data using IMOD. *J Struct Biol* 116:71–76
44. Mastronarde DN (2008) Correction for non-perpendicularity of beam and tilt axis in tomographic reconstructions with the IMOD package. *J Microsc* 230:212–217
45. Grant T, Grigorieff N (2015) Measuring the optimal exposure for single particle cryo-EM using a 2.6 Å reconstruction of rotavirus VP6. *elife* 4:e06980
46. Turoňová B, Schur FKM, Wan W, Briggs JAG (2017) Efficient 3D-CTF correction for cryo-electron tomography using NovaCTF improves subtomogram averaging resolution to 3.4 Å. *J Struct Biol* 199:187–195
47. Nicastrò D (2006) The molecular architecture of axonemes revealed by cryoelectron tomography. *Science* 313:944–948
48. Hrabe T et al (2012) PyTom: a python-based toolbox for localization of macromolecules in cryo-electron tomograms and subtomogram analysis. *J Struct Biol* 178:177–188
49. Bharat TAM, Scheres SHW (2016) Resolving macromolecular structures from electron cryotomography data using subtomogram averaging in RELION. *Nat Protoc* 11:2054–2065
50. Castaño-Díez D, Kudryashev M, Arbeit M, Stahlberg H (2012) Dynamo: a flexible, user-friendly development tool for subtomogram averaging of cryo-EM data in high-performance computing environments. *J Struct Biol* 178:139–151
51. Tang G et al (2007) EMAN2: an extensible image processing suite for electron microscopy. *J Struct Biol* 157:38–46
52. Galaz-Montoya JG, Flanagan J, Schmid MF, Ludtke SJ (2015) Single particle tomography in EMAN2. *J Struct Biol* 190:279–290
53. Carter SD et al (2018) Distinguishing signal from autofluorescence in cryogenic correlated light and electron microscopy of mammalian cells. *J Struct Biol* 201:15–25